ARTICLE OPEN

Check for updates

Adhesive free, conformable and washable carbon nanotube fabric electrodes for biosensing

Md. Milon Hossain[1,2], Braden M. Li[1,3,4], Busra Sennik[1], Jesse S. Jur[1] and Philip D. Bradford[1] ✉

Skin-mounted wearable electronics are attractive for continuous health monitoring and human-machine interfacing. The commonly used pre-gelled rigid and bulky electrodes cause discomfort and are unsuitable for continuous long-term monitoring applications. Here, we design carbon nanotubes (CNTs)-based electrodes that can be fabricated using different textile manufacturing processes. We propose woven and braided electrode design using CNTs wrapped textile yarns which are highly conformable to skin and measure a high-fidelity electrocardiography (ECG) signal. The skin-electrode impedance analysis revealed size-dependent behavior. To demonstrate outstanding wearability, we designed a seamless knit electrode that can be worn as a bracelet. The designed CNT-based dry electrodes demonstrated record high signal-to-noise ratios and were very stable against motion artifacts. The durability test of the electrodes exhibited robustness to laundering and practicality for reusable and sustainable applications.

npj Flexible Electronics (2022)6:97 ; https://doi.org/10.1038/s41528-022-00230-3

INTRODUCTION

Epidermal electronics have grown exponentially in the past decade with the advancement in miniaturized flexible and wearable bioelectronics. Such skin-attachable electronics are widely used in various human-computer interactions, augmented reality (AR) devices, and biomedical applications[1–4]. Electrophysiological monitoring (electrocardiogram-ECG, electromyogram-EMG, electroencephalogram-EEG, etc.) is a necessary sensing input needed to achieve these advanced applications. It is critical that these electrophysiological recordings acquire reliable and high-quality data points for health diagnosis in wearable biomedical applications like diagnosing nervous and cardiac systems[5]. The ionic movement, i.e., bioelectrical signal produced by myocardium, is converted into electron movement at the electrolyte–electrode interface, or electrode–skin interface, and this movement is recorded and expressed as voltage. The wet electrodes contain electrolyte (gel/adhesive) unlike dry electrodes and these pre-gelled Ag/AgCl electrodes (wet electrodes) are the gold standard for clinical ECG recordings[6,7]. An oxidation-reduction reaction takes place at the interface between Ag and electrolyte which facilitates the electrical transport. Therefore, wet electrodes are characterized by half-cell potential, capacitance and resistance[8]. Despite their outstanding signal quality, the electrolyte gel dries over time causing skin irritation, restricting long-term applications, and creates short-circuits in high density recordings[9–13]. Therefore, soft dry electrodes have emerged and exhibit improved wear comfort and reduction of skin irritation for long-term monitoring applications[14]. Dry electrodes could be surface electrode (direct contact with the skin), penetrating electrode (punch into the skin) and capacitive electrode (thin insulating layer separating skin and electrode)[15]. Surface electrodes are very common because of their noninvasive data acquisition. The coupling between skin and electrode for dry surface electrode is capacitive because of the absence of gel. However, high motion artifacts, low signal-to-noise ratios, and small coverage areas limit the applications of dry electrodes[16,17]. Generally, motion artifacts are prevalent for the thicker rigid dry electrode because this type of dry electrode cannot conform to the skin contour leading to air bubbles/gaps in between[15]. Therefore, dry electrodes are more susceptible to relative motion and friction between skin and electrodes resulting in signal instabilities and noise (low SNR)[18]. In addition, adhesive or straps are required for thicker film dry electrodes for reliable mounting on the skin[19]. Hence, much effort has explored the use of mechanically soft, thin films fabricated via structural engineering of rigid materials, to physically attach these films onto the skin by capillary or van der Waals interaction forces. However, such physical attachments are not robust and debond over time due to the dynamic environment of human skin[20,21]. Additionally, the rigidity of the materials in these films (i.e., thin metallics) results in high signal noise during body movement[22].

Textiles are ubiquitous to human life and being the closest layer to our body, they provide the ideal platform to develop sensing electrodes[23]. Textile-based electrodes can undergo complex and severe deformations (i.e., twisting, bending, stretching) while providing ultra-conformable and comfortable interfaces with human skin. Furthermore, the low bending stiffness and stretchability of previously reported textile electrodes enable reliable electrical performance[24–29]. Textile electrodes are skin-friendly and can be produced in large scale using conductive yarn by traditional knitting, weaving, embroidering, and braiding process[30,31]. Additionally, electroactive materials can be electroplated, printed, or coated on textiles to fabricate planar electrodes[32]. Advanced carbon materials, metallic nanoparticles, and conductive polymers are widely used for fabricating textile electrodes[22,33]. Among the carbon materials, carbon nanotubes (CNTs) demonstrate high aspect ratios, excellent mechanical properties, ultralight weight, and superb thermal and electrical properties[34,35]. However, most of the electrodes fabricated using CNTs are composite films and lack the breathability and comfort necessary for wearable applications[36–40]. Textile electrodes address these

[1]Department of Textile Engineering, Chemistry and Science, North Carolina State University, Raleigh, NC, USA. [2]Department of Mechanical and Aerospace Engineering, Cornell University, Ithaca, NY, USA. [3]Air Force Life Cycle Management Center, Human Systems Division, Wright-Patterson AFB, Dayton, OH, USA. [4]Air Force Research Laboratory, Materials and Manufacturing Directorate, Wright-Patterson AFB, Dayton, OH, USA. ✉email: philip_bradford@ncsu.edu

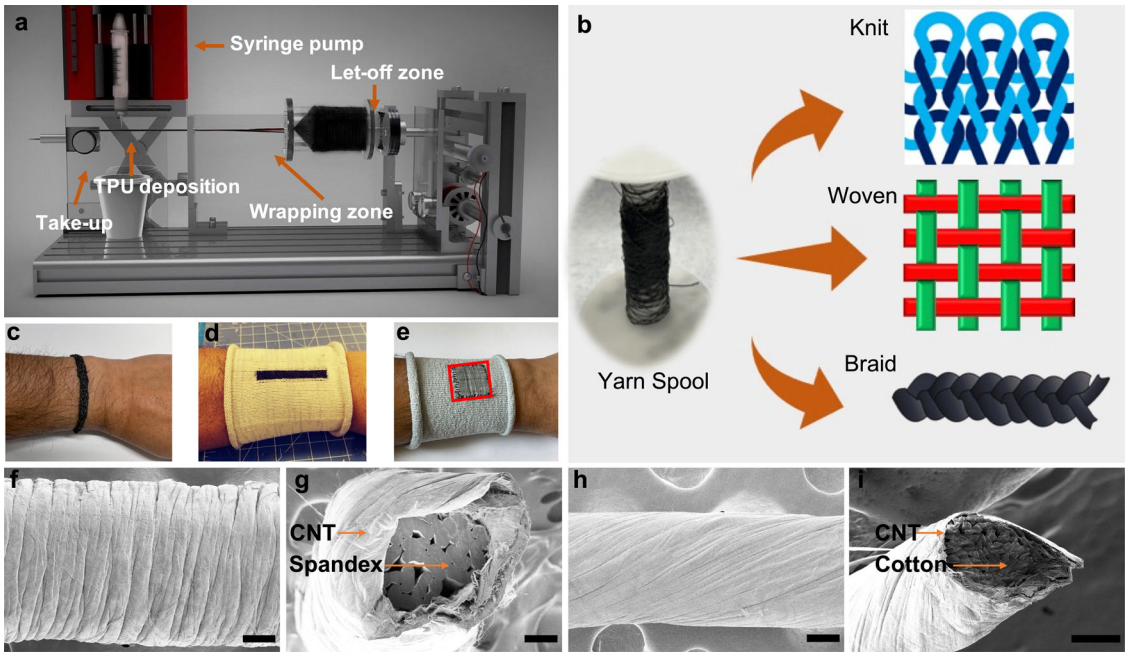

Fig. 1 CNT Yarn and Textile Fabrication. a Fabrication schematic of the CNT wrapped textile yarn spinning system. Two CNT sheets are attached in the let-off zone and wrapped over core yarn in the wrapping zone. TPU is deposited on the CNTs wrapped yarn surface before winding in take up roller. **b** Different textile processing methods for producing fabric electrodes. The inset shows a spool of CNT wrapped yarn used for the electrodes. Fabric electrodes produced including **c** braided **d** knitted and **e** woven electrode (outlined in red) sewn on a wrist band **f**–**i** The surface and cross-sectional morphology of the CNT-Spandex-TPU (Fig. 1f, g) and CNT-Cotton-TPU (Fig. 1h, i). The scale bar of the SEM images are 100 microns.

issues as they are highly porous and flexible making them suitable for long term skin contact applications. Besides, it is easy to produce different designs by varying the multiple color combinations, pattern, and styles[34]. Recently, CNT thread electrodes were sewn into a garment and exhibited comparable ECG signals to commercial electrodes[41]. However, the poor elongation (~2%) would restrict that yarn from many textiles manufacturing processes, especially knitting. Moreover, sewing is a comparatively lengthy process for large area and bulk scale manufacturing compared to other textile processing methods like knitting, weaving, and braiding. Therefore, there exists a critical need to develop conductive yarns with higher elongation for sustainable fabrication and design of textile electrodes. The creation of large area and seamless textile electrodes demands innovative fabrication processes utilizing CNT yarns.

Here, we offer a comprehensive solution for dry ECG electrodes through multiple fabric structures produced with commercial textile manufacturing processes. We first developed a textile processable conductive yarn by wrapping CNTs over cotton and spandex yarns, respectively, in a core-sheath structure. The cotton yarns are the most commonly used textile fibers due to their softness, biodegradability, breathability, and low cost[42]. The spandex core imparts high stretchability to the yarns and combined with the fabric structure, can offer ultra-conformability with the skin, preventing deformation induced motion artifacts. Three different fabric structures: knit, woven and braid are demonstrated in this work. Each provides unique stretch and comfort characteristics allowing the properties to be tuned for varying application scenarios. For example, fabric electrodes for daily indoor use may be designed with low stretch needs while electrodes used during athletic activities may be designed with much higher extensibility requirements. No adhesive or support structure are required for our textile electrodes to collect reliable ECG data and could be worn and washed as a regular textile-based devices without encapsulation. We demonstrated that the fabric-based electrodes recorded comparable ECG signals (with similar signal-to-noise ratios) to that of standard, commercial Ag/AgCl electrodes in both static and dynamic conditions.

RESULTS AND DISCUSSION

Textile electrode fabrication and characterization

CNT wrapped cotton and spandex yarn were fabricated using the custom-built spinning device shown Fig. 1a. First, two CNT arrays were mounted on the let-off zone of the spinning device. Core cotton and spandex yarns were inserted through the inner tube of the let-off cylinder. The core inserting inner tube has a diameter of 0.5 cm to accommodate a wide variety of textile yarns. To ensure smooth feeding of the core yarn, a spring tensioning system was used to control the tension. The aligned CNTs sheets were directed through a guide on the let-off cylinder and densified into a ribbon. Because this CNT ribbon lacked twist, it had low fiber-fiber interaction, resulting in low strength[43]. The CNTs sheet were then wrapped over the core yarn and twist was introduced during the wrapping process that can be seen in Supplementary Video 1. The resultant core-sheath yarn was a cylindrical shape with increased packing density induced by the wrapping/twist process. Then 1% TPU binder was applied before collecting the yarn on a spool (Fig. 1b). We did the initial study to observe the impact of TPU concentration on the resistance and surface smoothness of the yarn. We found that increasing the TPU concentration increases the resistance of the yarn. The relationship between TPU% and changes in resistance is presented in Supplementary Fig. 2. Yarns with 1% TPU have better surface smoothness (Supplementary Fig. 3) than others and the lower TPU% evaporates quickly in air without additional drying system for TPU. Therefore, we selected 1% TPU for the rest of our experiment. The diameters of the cotton and spandex yarn were 260 microns and 450 microns whereas CNT-Cotton-TPU and CNT-Spandex-TPU yarn were around 332 and 507 microns, respectively. The core-sheath yarns were used in fabric-based wrist electrodes produced using weaving, knitting and braiding and are presented in

Fig. 1c–e. While braided (Fig. 1c) and knitted (Fig. 1d) electrodes were self-supported, the woven (Fig. 1e) electrode was sewn onto a wristband. The morphologies of the CNT-Spandex-TPU and CNT-Cotton-TPU yarn's surface and cross-section are presented in Fig. 1f–i. The cross-sections of the yarns show the wrapping of CNTs around the core yarn.

Yarn flexibility and stretchability are critical for textile manufacturing and wearable electrode applications. Electrodes or devices used for wearable applications may experience up to 20% strain during body movement, based on its position on the body[44]. Textile manufacturing processes require yarns that can resist twisting, bending and frictional forces. As such, it is essential to evaluate the electromechanical performance of the yarns. The CNT-Spandex-TPU yarns exhibited lower elastic moduli and tensile strengths compared to the CNT-Cotton-TPU yarn (Supplementary Fig. 4a). The tensile curves for the both yarns are non-linear and the curves increase gradually at lower strain (Supplementary Fig. 4b, c) and the slopes fluctuate as the strain increases. Under the load, the CNTs are stretched and the fraction of load-bearing CNTs increases with tension. The abrupt changes in slopes at mid-higher strain is because of the largest relative fraction of CNTs is load bearing. The second peak at the highest strain is contributed by the core yarn. This tensile behavior for CNTs was reported by different researchers[45–47]. As expected, the CNT-Cotton-TPU yarns failed at ~10% strain (Supplementary Fig. 4b) because of comparatively low elasticity of core cotton yarn than spandex. On the other hand, the stress–strain curve of the CNT–Spandex–TPU yarns showed very high stretchability (~100% failure strain) (Supplementary Fig. 4c). The mechanical properties of textile fabrics are a function of both the yarn type and fabric construction. However, the stability of the yarns under different mechanical deformations such as bending and twisting was evaluated (Supplementary Fig. 5) for device fabrication using textile technology. Bending both yarns at 30–90° degrees did not show any significant change in resistance. The yarn also demonstrated excellent robustness against twisting indicating their suitability for the device fabrication. Electromechanical behavior of CNT yarn is greatly influenced by the twist and pretension during the test. Interestingly, the electromechanical behaviors of the yarns revealed opposite trends in resistance change at low strain (Supplementary Fig. 4d, e). The spandex core in the CNT–Spandex–TPU yarns allowed higher extensibilities, but the CNT–Cotton–TPU yarns showed lower relative resistance changes. The core cotton yarn has lower extensibility and thus a small change in resistance was observed for the CNT-Cotton-TPU yarn. The changes in resistance of the yarns at strain range 0–5% are compared in Supplementary Fig. 4f and both a negative and positive resistance response were recorded. There could be two possible reasons for this different behavior in resistance change. First, pre-tensioning the samples during mounting to the tensile tester does not show negative resistance change. Because of highly stretchable spandex core, the sample was straightened out/pretensioned before starting the tensile test and thus showed positive resistance change. Secondly, the CNT–Cotton–TPU and CNT–Spandex–TPU yarn have different wrapping angle (Fig. 1f, h) of around 20° and 80°, respectively depicting the different alignment of CNTs. The larger wrapping angle for CNT-Spandex-TPU provides more space to readjust the fiber alignment during loading unlike CNT–Cotton–TPU. Comparatively, parallel alignment of CNT–Cotton–TPU experiences more lateral contraction at low strain during loading which increases inter-tube contact area leading decrease in resistance[43]. The lateral contraction reaches the threshold strain of 3% (lowest resistance) and resistance reverts to an increase with the increasing strain%. The CNT wrapped yarn was used for producing different type of electrodes for ECG application by weaving, knitting and braiding process as shown and discussed in Supplementary Fig. 1 and Supplementary Method 1.

The geometry and surface characteristics of the different electrodes are presented in Fig. 2a–f. The woven fabric (Fig. 2a)

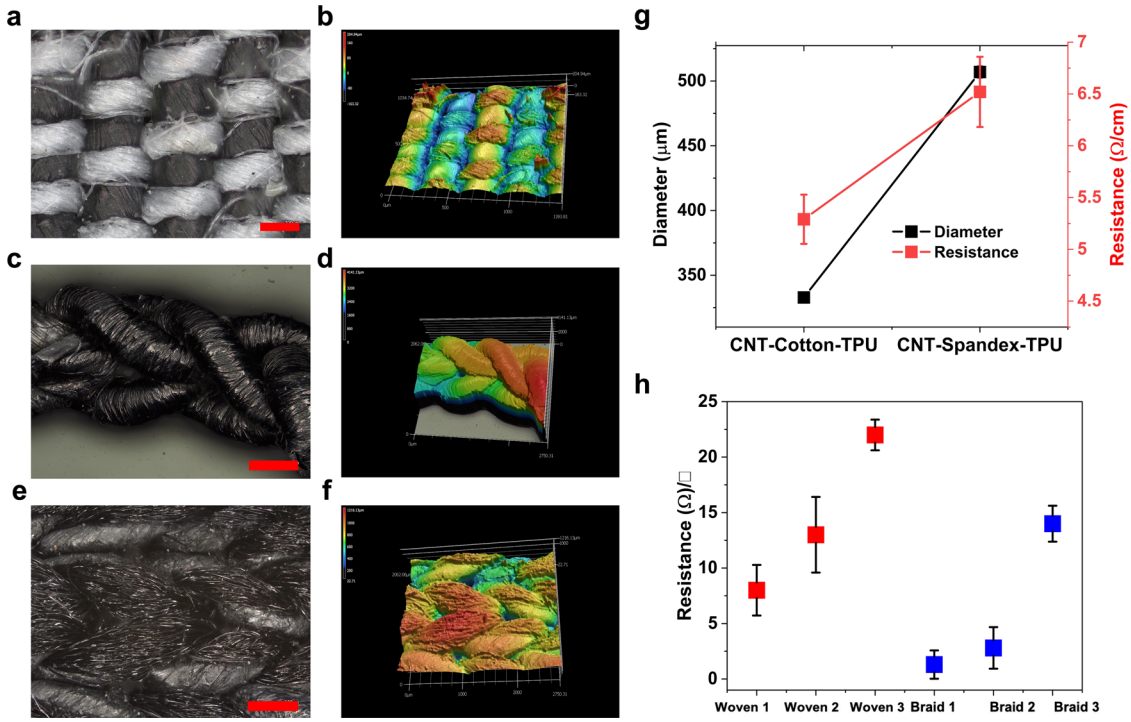

Fig. 2 Morphological and Electrical Characteristics of CNT Textile Electrodes. a Optical microscopic images of the **a** woven, **c** braid, **e** and knit electrodes with corresponding laser profiling images of the **b** woven, **d** braid and **f** knit electrode textile structures. Electrical resistance and diameter of the **g** CNT wrapped yarns and electrical resistance of **h** CNT textile electrodes. Data are presented as mean ± SD. The scale bar of the images are 200 microns **a** and 500 microns **c**, **e**.

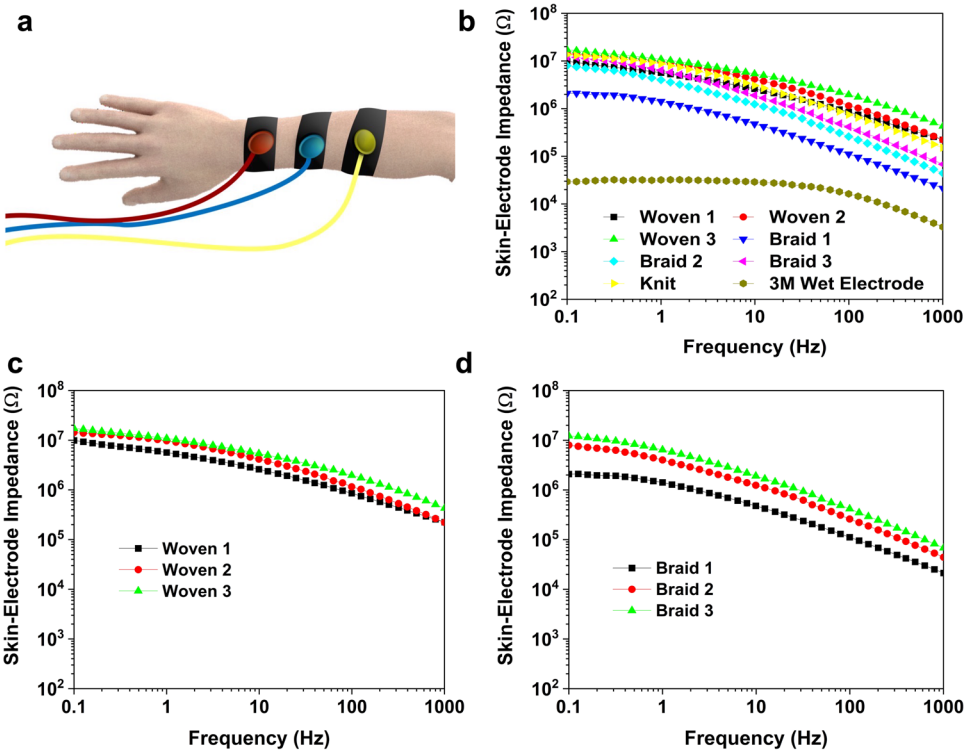

Fig. 3 Impedance Analysis of CNT Textile Electrodes. a Electrode placement for impedance measurements. **b** Impedance characteristics of CNT textile electrodes compared to commercial wet electrodes. Impedance variations against different size of **c** woven electrodes (CNT–Cotton–TPU yarn is in weft direction and neat cotton in warp direction. The electrode contains equal number of CNT-Cotton-TPU and neat cotton yarn per unit area. The electrode size decreases from Woven 1 to Woven 3. **d** braided electrodes contains all CNT–Spandex–TPU yarn intertwined together. The electrode size decreases from Braid 1 to Braid 3.

contains CNT–Cotton–TPU yarns in the weft (horizontal) direction and cotton yarns in the warp (vertical) direction. The woven textile electrodes have good dimensional stability, and the inelastic behavior of the structure does not change the resistance under tension. While the woven electrodes might be suitable for relaxed conditions or low body movement conditions, it is not preferred electrode structure for large body movement conditions.

Braiding is the simplest design process and can produce compact structure. However, they are the most rigid structure and therefore, CNT yarn containing highly elastic spandex yarn were used for designing braided electrode. Three CNT–Spandex–TPU yarns were interlaced to produce braided structures and repeated to increase the width of the braid (Fig. 2c). The braid structures contained the highly stretchable CNT–Spandex–TPU (Supplementary Fig. 6) yarns allowing the braid to be stretched over 100% which is multiple times higher than the maximum strains observed in body movement. Intermeshing of loop called knitting is known for their superior conformability, comfort, stretchability, and rapid prototyping[48,49]. A rib knit structure (Fig. 2e) was chosen due to their high structural stability compared to jersey structure. Besides, rib structures can prevent motion artifacts better than jersey structure due to their comparatively better stability under stress. The order of comfortability and wearability are knit>woven> braid structures according to the shear and bending stiffness[50]. Though the knit structure was produced using a cotton core, it also showed a high stretchability of 70% due to knit geometry (Supplementary Fig. 6). Knits are inherently more stretchable than braids or woven fabrics (which typically have straight yarns) because their structure contains loops. Both our yarn and fabric electrodes showed higher extensibility compared to other reported CNT–yarn ECG electrodes[41]. The electromechanical properties of the electrodes are discussed and shown in Supplementary Discussion 1 and Supplementary Fig. 7.

Yarn diameter is directly related to the yarn linear density and defines the knittability. For example, a typical rib knit structure requires yarn linear density of 12–20 tex to be processed with commercially standard 15-gauge weft knitting machines[51]. Unlike other yarn fabrication processes, this innovative wrapping process eliminates the separate processing steps such as multiplying CNT yarn, densification etc. to produce high linear density yarn required for textile processing[41,52]. The linear density of the yarn increased significantly by 75% for CNT–Cotton–TPU (35 Tex) and 33% for CNT–Spandex–TPU (146 Tex) which is crucial for textile processing[53]. Low yarn linear densities produce unstable and defective knit fabrics and high linear densities may damage the knitting needles. The yarn's diameter and electrical resistance are presented in Fig. 2g. CNT–Spandex–TPU has higher diameter above 500 microns resulting from 110 Tex core spandex. The resistance is also higher for CNT–Spandex–TPU yarn due to the more radial alignment of CNT along the yarn axis compared to the CNT-Cotton-TPU. This resulted in a higher resistance change for CNT–Spandex–TPU yarn (Supplementary Fig. 4e). Under tension, the radial yarns align themselves with the yarn axis and affect the electrical conductivity. Compared to the CNT multiplying process, CNT wrapping process eliminates the laborious processing steps and makes the process faster[41]. The resistances of the woven and braided electrodes are directly related to the electrode size. With the increase of electrode size, more CNTs are interconnected, and the resultant resistance decreases (Fig. 2h).

Impedance behavior

The placement of electrodes used in impedance measurements is presented in Fig. 3a. The interfacial impedance between the skin and electrodes collected from the arm (Fig. 3b). The electrode impedance varies according to electrode designs and sizes. All of the fabric electrodes used were in the form of a wrist band.

The braided structures had comparatively lower skin-electrode impedance compared to woven and knitted ones. Both the woven and braided electrodes demonstrated a direct relationship between electrode size and impedance and skin-electrode impedance decreases with increasing electrode size (Fig. 3c, d). In the case of woven electrodes, increasing the size slightly reduces the impedance because the woven electrode contains insulating cotton yarns. In contrast, there is a correlation between textile electrodes and the amount of conductive materials in contact with the skin. Besides, the contact pressure also influences the skin-electrode impedance[54]. Unlike woven electrodes, braided electrodes contain all CNT yarn and demonstrated direct correlation between electrode size and impedance (Fig. 3d). With the higher electrode size (Braid 1), skin-electrode contact impedance decreases as reported in other study[36]. Compared to 3M wet electrodes, textile electrodes have higher skin-electrode impedance due to the lack of ionic conductivity. In dry electrodes, the signal is transferred by only electrical conductivity[55]. However, the biosensing performance of the electrodes were not affected by the lower impedance compared to the 3M wet electrode. All the electrodes exhibited decreasing trend in impedance with the frequencies. Braid 1 electrode has the lowest impedance of 112 kΩ at 100 Hz better than the impedance of CNT yarn electrode[41].

ECG analysis and monitoring

Electrode design plays an important role obtaining high-fidelity ECG signals from dry electrodes. Most dry electrodes suffer from motion artifacts and are susceptible to environmental conditions such as washing. The setup for ECG data recording is shown in Fig. 4a, b and Supplementary Video 2 where 3M electrodes were used as the control measurement. An extract of 10 s from the ECG recording of each electrode exhibited easily distinguishable P–QRS–T complexes (Supplementary Fig. 8). However, the peak amplitude was affected by the active electrode area. A comparison between the 3M electrode and Woven 3 showed similar ECG signal demonstrating the high quality of the designed fabric CNT electrode (Supplementary Fig. 9a). Similar results were also found for Braid 1 (Supplementary Fig. 9b). To further investigate the real-world usability of the fabric CNT electrodes, another test was conducted where counter and reference 3M electrodes were replaced with braided CNT electrodes (all three electrodes being braided) with the recorded ECG data presented in Fig. 4c. The ECG signal remained as high quality and very comparable to the data collected with 3M wet counter and reference electrodes. The comparable performance of fabric CNT ECG electrodes is due to high skin conformability of the electrodes. Skin contact greatly influences the ECG signal quality[56]. Braided electrodes were stretched to be placed on the wrist as a bracelet, and the compressive force of the bracelet provided the close contact with the skin enabling the electrode to capture high quality ECG data. Most of the dry electrodes found in literature are designed as a thin film on plastic backing which provide smaller surface contact area due to the unevenness of skin. As a result, a portion of the signal from the skin does not completely transfer to those type of electrodes[54].

Knitted fabrics are more flexible and conformable to the body and it is the reason they are most often used for athletic wear and compression garments. Thus, it was expected that our knitted electrodes would perform better than woven electrodes. The signal to noise ratio (SNR) of the electrodes are presented in Fig. 4g, h and compared with the commercial electrode. The SNR of electrodes are greatly affected by the electrode size, design and manufacturing methods. SNR decreases with the size of woven electrode while increases for braided electrode. This is due to the changes in active electrode area per unit. Despite the high resistance of Braid 1 compared to Braid 3, the high porosity (Supplementary Fig. 10) of Braid 3 might decrease the SNR. However, low resistance is not the only criteria for an electrode to perform better during ECG signal recording and it is unknown if the ECG signal depends only on low skin-electrode impedance[18,57]. The braided electrodes were mounted on the skin without controlling the adhesion force and might have different skin contact pressure contributing to unwanted noise during ECG recording and differences in SNR was observed. On the other hand, Woven 3 has lower active electrode per unit compared to Woven 1 resulting in decrease in SNR. Despite their variation in SNR, they are indistinguishable compared to the SNR of 3M electrode except Woven 3.

The ECG recording of the electrodes were collected in three different body movement conditions walking at 2 mph, jogging at 4 mph and running at 6 mph (Fig. 4d–f). The difference in peak shape was because of the orientation of the electrodes (connection of leads to the specimen) during measurements. The ECG waveforms are distinguishable during walking and jogging conditions. However, noise appears in the ECG signal with the increase of movement. The baseline wander is mostly caused by the contact instability because the freestanding Braid 1 and knit wristband were placed on the arm at low contact pressure. On the other hand, a pressure band was used with the Woven 3 and comparatively a stable baseline was observed[29,58]. The slight change in baseline wander appears due to the respiration[54]. Comparatively, Woven 3 and knit wristband demonstrated high stability against motion artifact than Braid 1. Though the 3M wet electrode performs slightly better against motion artifacts[59], introduction of noise and baseline wandering is common issues for both dry and wet electrodes for ambulatory ECG recording. However, 3M wet electrodes are not suitable for long-term and reusable application because of drying out of the gel. Additionally, they are susceptible to washing and bending and deteriorates the ECG signal quality[38,60].

While the ECG signal obtained by CNT textile electrodes are comparable to the 3M electrodes, CNT textile electrodes are advantageous because: CNT textile electrodes are reusable, and the signal quality does not degrade over time and has smaller electrochemical noise[61]. The 3M electrodes are susceptible to mechanical bending and demonstrates lower performance[60]. It is important to note that, all the ECG data recorded over 2 months using the CNT textile electrodes and the electrodes were subjected to severe folding and bending. However, all the data were consistent without any changes demonstrating their excellent resistance to regular handling of the CNT textile electrodes.

Wash durability characteristics

Numerous reports have demonstrated high fidelity of electrophysiological signals using different electrode materials. However, very few have tested their electrodes for wash durability (Supplementary Table 1). Wash durability is critical for long-term and sustainable application of dry ECG electrodes. The idea being that these non-intrusive electrodes could be used numerous times in a home or institutional healthcare setting without being thrown away. Figure 5 shows the ECG signals of our CNT-based textile electrodes after numerous washing cycles (as defined in the experimental section). The ECG signals after 5 washing cycles are very stable and comparable with the unwashed 3M wet electrode (Fig. 5a). Both electrodes demonstrated comparable ECG signals after washing. It is very important to identify R peak to detect various health abnormalities. An instantaneous heart rate could be obtained by properly detecting R-R peak intervals[62]. To better evaluate the washability of the CNT-based dry electrodes, the R to S peak amplitude was compared to unwashed 3M wet electrode (Fig. 5b). Both the woven and braided electrode demonstrated higher R to S peak amplitude compared to 3M wet electrode. A slight decrease in R to S peak amplitude was observed after 5

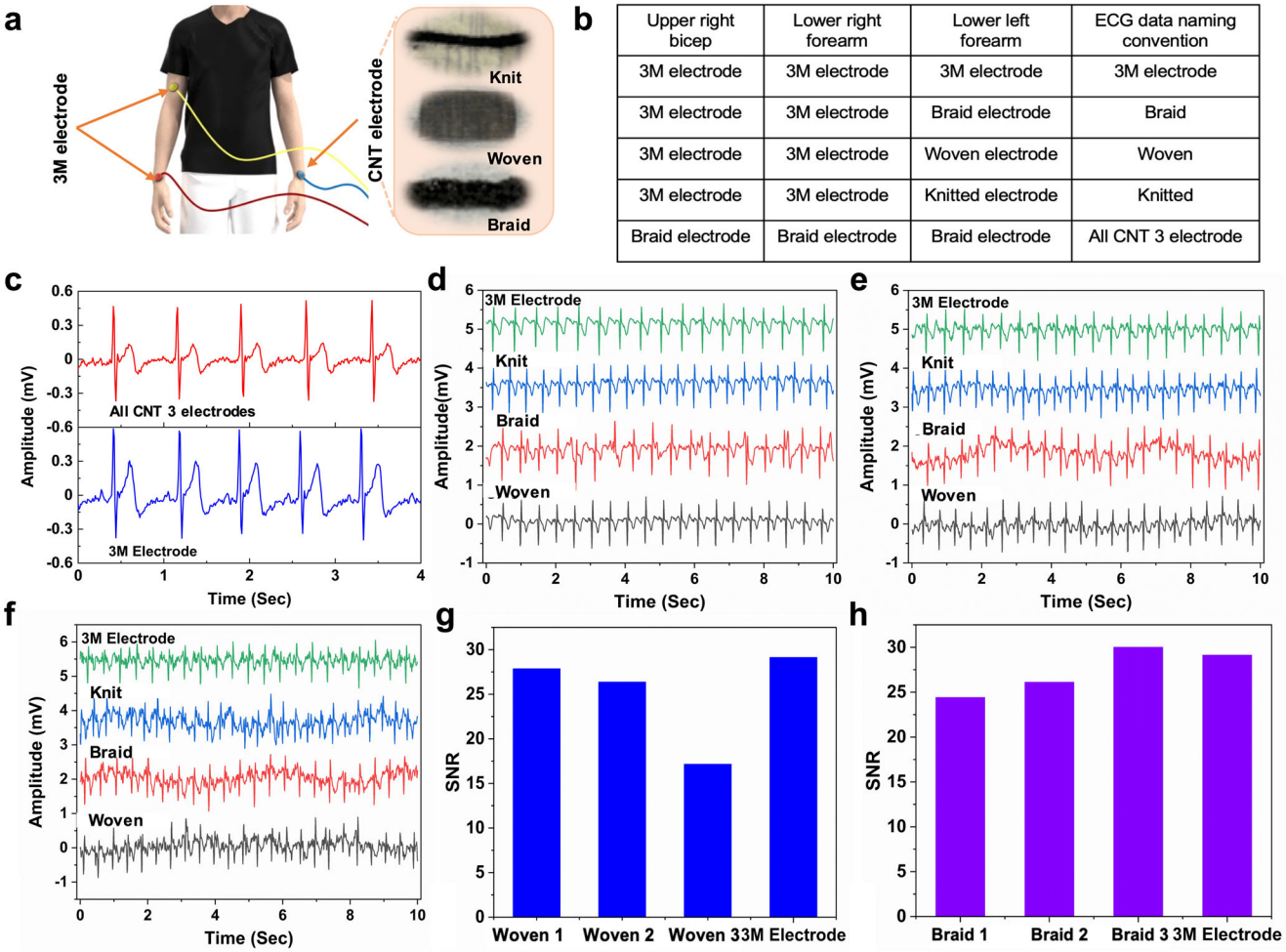

Upper right bicep	Lower right forearm	Lower left forearm	ECG data naming convention
3M electrode	3M electrode	3M electrode	3M electrode
3M electrode	3M electrode	Braid electrode	Braid
3M electrode	3M electrode	Woven electrode	Woven
3M electrode	3M electrode	Knitted electrode	Knitted
Braid electrode	Braid electrode	Braid electrode	All CNT 3 electrode

Fig. 4 Electrocardiogram Sensing Performance of CNT Textile Electrodes. a Electrode placement for ECG recording **b** variation of lead positions and naming convention **c** ECG signal comparison between all carbon electrode (three braided electrodes were used-top) and commercial 3M wet electrode (bottom) ECG signal comparison from walking to running movements with **d** 2 mph **e** 4 mph and **f** 6 mph of movement speed. Comparison of SNR at static condition against different electrode sizes **g** woven electrodes **h** braided electrodes.

washing that is still higher than unwashed 3M electrode. The R to S peak amplitude was higher for Braid 2 compared to Woven 2 electrode. Though the R to S peak amplitude of Braid 2 and Woven 2 electrodes decreased after 10 washings, the P-QRS-T waveforms are clearly distinguishable. The characteristics waveforms after different washing were further confirmed by analyzing overlaid single waveforms in Supplementary Fig. 11. The orientation of Q-wave, R-peak, and S-wave are visible after 5 (Supplementary Fig. 11a) and 10 washing (Supplementary Fig. 11b). However, the electrode configuration during measurement resulted in inverted T-wave[63]. The decrease in R to S peak amplitude after 10 washing could be due to some surface damage caused by the friction of metal balls used during washing. Though no rupture or severe damage on the device surface was observed (Supplementary Fig. 12), some reorientations of CNTs on the device surface were observed which might affect the ECG data recording. However, polymer encapsulation or sealing the device could improve the wash durability for longer cycles[64].

The electrodes were further washed to evaluate their durability and reusability and the resistance changes of the electrodes before and after 25 washing was negligible (Supplementary Fig. 13). In comparison to commercial wet electrodes, which start to degrade after 6 h of use (due to the gel drying out), our fabric electrodes retain the similar performance even after many washing cycles. Thus, the electrodes could be reused over time, making them not only more convenient but also possibly more affordable. The performance of our fabric electrodes was compared to other textile based dry electrodes from the literature (Supplementary Table 1) and showed superior performance retention after washing.

Most of the dry ECG electrodes are fabricated on/in a substrate with limited flexibility. Fabric based electrodes are desirable for wearability, comfort and skin contact. Here, we demonstrated the fabrication of fabric-based ECG electrodes using CNTs wrapped textile yarns. We utilized these yarns with commercially available textile manufacturing equipment and successfully designed woven, knit and braid electrodes. We showed that high-fidelity ECG signals could be recorded using these electrodes which were comparable to conventional wet electrodes (3M Red Dot) including their SNR. The electrodes are stable during body movement and produced distinguishable P-QRS-T ECG signals. The knitted wristband demonstrated highly advanced seamless fabrication without affecting the comfort and typical characteristics of textiles. This allows the electrode to be mounted on the skin as a regular textile for long term monitoring. Finally, we demonstrated that the electrodes are highly durable to washing and could be washed in commercial laundry without affecting the signal quality. In future studies, the impact of different knit design and woven electrode produced entirely of CNTs would be evaluated for ECG data recording.

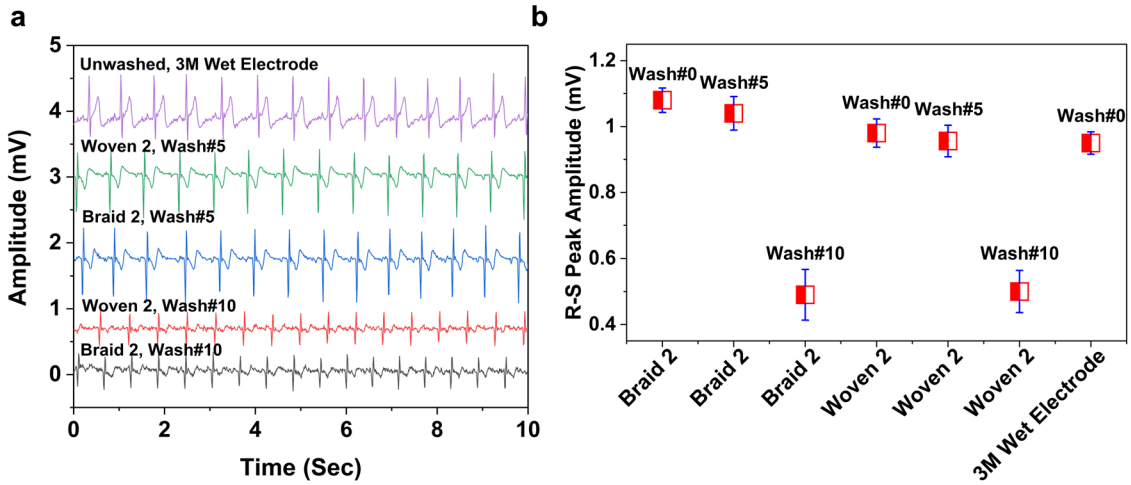

Fig. 5 Wash Durability of CNT Textile Electrodes. ECG signals after **a** different washing **b** R-S peak amplitude before and after washing. Data are presented as mean ± SD.

METHODS

CNT synthesis

Multi-walled carbon nanotubes (MWCNTs) were grown vertically on a quartz substrate using a catalytic chemical vapor deposition method. Average CNT diameter of ~30 ± 8 nm and length of ~1 mm was obtained. Iron II chloride ($FeCl_2$) was used as the catalyst and acetylene as a precursor gas for CNTs. The arrays were grown at 760 °C and 5 Torr under acetylene (600 sccm), argon (400 sccm), and chlorine (2 sccm) flow. The growth process was carried out for 20 min and then the acetylene was purged during the cool down. Detail of this synthesis process has been reported in our previous works[65–67]. The vertical alignment of the CNT within the arrays enabled continuous drawing of the CNTs into a low density, horizontally aligned CNT sheet.

CNT wrapped textile yarn fabrication

The yarn spinning process was initiated by dragging a razor blade across one edge of the CNT array to form the CNT sheet. Then these two aligned CNTs arrays were placed on a rectangular rotating cylinder opposite to each other (see Fig. 1a). Next, the CNT sheets were pulled through a guide and wrapped together over a core yarn consisting of either cotton or spandex. The linear densities of the cotton and spandex yarns were 20 and 110 Tex (weight in grams per kilometers) respectively. The resultant core-sheath yarn was continuously wound on a cylinder. Next, a thermoplastic polyurethane (TPU, Desmocoll 530, Bayer Material Science) solution dissolved in acetone was applied to the yarn surface at a rate of 0.3 µL per min by a syringe pump. The yarn was then transferred to a spool for further textile processing into fabric electrodes.

Designing biosensing electrodes

Different textile structures were produced using the CNT wrapped core-sheath yarns. CNT wrapped spandex yarn was used to produce three braids with dimensions 6 in ×0.03 in (Braid 1), 6 in ×0.011 in (Braid 2), and 6 in ×0.004 in (Braid 3). CNT wrapped cotton yarns were used as weft yarn for producing woven fabrics. Three samples with sizes of 7.1 cm^2 (Woven 1), 5.8 cm^2 (Woven 2) and 3.2 cm^2 (Woven 3) were produced using a semi-automatic shuttle weaving machine. A plain woven (1/1) structure was produced with the construction of 80 warp and 60 weft yarns per inch. Knitted electrodes used CNT-Cotton-TPU yarns to produce a fabric electrode and denoted as Knit. A seamless wristband was programmed and simulated in Shima Seiki's SDS-ONE Apex3 design system and knitted on a Shima Seiki SWG061N2 (15 gauge) Whole Garment flat knitting machine. The knitting parameters were adjusted based on the design of the knit structure and the knitting speed was 0.8 m/s. The CNT-Cotton-TPU yarn was integrated continuously using an intarsia pattern, whereas the base yarn of the wrist band was cotton yarn. More details about the three different design of textile electrodes can be found in Supplementary Method 1 and Supplementary Fig. 1.

Characterization of electrodes

The yarn surface characteristics were imaged using a field emission scanning electron microscope (SEM), FEI Verios 460 L, at a 2 kV beam voltage and 13 pA beam current. The diameter of the core-sheath yarns were taken from SEM images, processed using NIH Image J software. The surface images and topographic profile of the specimens were visualized through 3D laser scanning confocal microscopy (Keyence, model VK-X1000). The electromechanical properties of CNT-Cotton-TPU and CNT-Spandex-TPU were investigated by combining tensile data from a MTS Criterion Model 43 and Keysight multimeter. The samples had a 40 mm gauge length, and the test speed was 30 mm/min.

Electrical impedance measurements

Electrical impedance of the electrodes were determined using a Gamry Instruments Interface 1010 E. Data were obtained at a frequency sweep from 0.1 to 1000 Hz at 10 mV. A three-electrode configuration was used where 3M wet electrodes (3 M™ 2560 Red Dot™) were used as reference and counter electrodes. The working electrodes were the different textile structures containing CNT core-sheath yarns. All electrodes were placed on the subject's left forearm at an 8 cm equilateral distance.

Electrocardiogram measurements

Electrocardiography data were recorded using BioPac MP160 system interface with a ECG100C wired amplifier at a sampling rate of 100 Hz. The ECG100C amplifier used a normal mode setting, 2000 gain, 35 Hz low pass filter, and a 0.05 Hz high pass filter. The electrodes were placed on the lower left forearm, upper right bicep, and lower right forearm for measurements using the same electrode configurations mentioned in the previous section. The measurements of the CNT textile electrodes were taken without any skin preparation or application of any gels. Plotted ECG data in manuscript is raw data originating from the BioPac system. The obtained ECG data were analyzed for SNR and filtered using a 0.5 Hz low pass filter to remove baseline wander noise using MATLAB R2021a software (MathWorks).

For the SNR calculations, first a custom MATLAB code identifies the QRS complex followed by determination of the P- and T-waves locations and amplitudes. Then the determined P-QRS-T complex is subtracted out from the ECG signal. The remaining components left in the ECG signal define the noise while the P-QRS-T complex defines the signal contribution for the final SNR calculation.

Washability testing

The Woven and Braid textile electrodes were washed according to the AATCC test standard TM 61-1A Test Method for Colorfastness to Laundering: Accelerated[68]. The specimens were placed in a beaker with 200 ml water and 10 steel balls were added. The standard AATCC detergent was also used as per the test requirement. The washing cycle ran for 45 min at 40 °C. After each washing cycle, the fabric containing CNT yarn was dried in the oven at 100 °C for 60 min.

DATA AVAILABILITY

The datasets generated and analyzed during the current study are available from the corresponding author on reasonable request

Received: 9 August 2022; Accepted: 14 November 2022;
Published online: 09 December 2022

REFERENCES

1. Son, D. et al. An integrated self-healable electronic skin system fabricated via dynamic reconstruction of a nanostructured conducting network. *Nat. Nanotechnol.* **13**, 1057–1065 (2018).
2. Gao, Y., Yu, L., Yeo, J. C. & Lim, C. T. Flexible hybrid sensors for health monitoring: materials and mechanisms to render wearability. *Adv. Mater.* **32**, 1902133 (2020).
3. Yamamoto, Y. et al. Efficient skin temperature sensor and stable gel-less sticky ECG sensor for a wearable flexible healthcare patch. *Adv. Healthc. Mater.* **6**, 1700495 (2017).
4. Kim, T., Park, J., Sohn, J., Cho, D. & Jeon, S. Bioinspired, highly stretchable, and conductive dry adhesives based on 1D-2D hybrid carbon nanocomposites for all-in-one ECG electrodes. *ACS Nano* **10**, 4770–4778 (2016).
5. Liu, Y. et al. Soft conductive micropillar electrode arrays for biologically relevant electrophysiological recording. *Proc. Natl Acad. Sci. USA* **115**, 11718–11723 (2018).
6. Huang, C. Y. & Chiu, C. W. Facile fabrication of a stretchable and flexible nanofiber carbon film-sensing electrode by electrospinning and its application in smart clothing for ECG and EMG monitoring. *ACS Appl Electron Mater.* **3**, 676–686 (2021).
7. Sinha, S. K. et al. Screen-printed PEDOT:PSS electrodes on commercial finished textiles for electrocardiography. *ACS Appl Mater. Interfaces* **9**, 37524–37528 (2017).
8. Fu, Y., Zhao, J., Dong, Y. & Wang, X. Dry electrodes for human bioelectrical signal monitoring. *Sens. (Switz.)* **20**, 3651 (2020).
9. Zhao, Y. et al. Ultra-conformal skin electrodes with synergistically enhanced conductivity for long-time and low-motion artifact epidermal electrophysiology. *Nat. Commun.* **12**, 4880 (2021).
10. Qiu, J. et al. A bioinspired, durable, and nondisposable transparent graphene skin electrode for electrophysiological signal detection. *ACS Mater. Lett.* **2**, 999–1007 (2020).
11. Ferrari, L. M. et al. Ultraconformable temporary tattoo electrodes for electrophysiology. *Adv. Sci.* **5**, 1700771 (2018).
12. Leleux, P. et al. Ionic liquid gel-assisted electrodes for long-term cutaneous recordings. *Adv. Healthc. Mater.* **3**, 1377–1380 (2014).
13. Fayyaz Shahandashti, P., Pourkheyrollah, H., Jahanshahi, A. & Ghafoorifard, H. Highly conformable stretchable dry electrodes based on inexpensive flex substrate for long-term biopotential (EMG/ECG) monitoring. *Sens Actuators A Phys.* **295**, 678–686 (2019).
14. Stauffer, F. et al. Skin conformal polymer electrodes for clinical ECG and EEG recordings. *Adv. Healthc. Mater.* **7**, 1700994 (2018).
15. Yao, S. & Zhu, Y. Nanomaterial-enabled dry electrodes for electrophysiological sensing: a review. *JOM* **68**, 1145–1155 (2016).
16. Wang, Y. et al. Electrically compensated, tattoo-like electrodes for epidermal electrophysiology at scale. *Sci. Adv.* **6**, eabd0996 (2020).
17. Ershad, F. et al. Ultra-conformal drawn-on-skin electronics for multifunctional motion artifact-free sensing and point-of-care treatment. *Nat. Commun.* **11**, 3823 (2020).
18. Chi, Y. M., Jung, T. P. & Cauwenberghs, G. Dry-contact and noncontact biopotential electrodes: methodological review. *IEEE Rev. Biomed. Eng.* **3**, 106–119 (2010).
19. Nawrocki, R. A. et al. Self-adhesive and ultra-conformable, Sub-300 nm dry thin-film electrodes for surface monitoring of biopotentials. *Adv. Funct. Mater.* **28**, 1803279 (2018).
20. Sim, K. et al. An epicardial bioelectronic patch made from soft rubbery materials and capable of spatiotemporal mapping of electrophysiological activity. *Nat. Electron* **3**, 775–784 (2020).
21. Deng, J. et al. Electrical bioadhesive interface for bioelectronics. *Nat. Mater.* **20**, 229–236 (2021).
22. Zhang, L. et al. Fully organic compliant dry electrodes self-adhesive to skin for long-term motion-robust epidermal biopotential monitoring. *Nat. Commun.* **11**, 4683 (2020).
23. Wicaksono, I. et al. A tailored, electronic textile conformable suit for large-scale spatiotemporal physiological sensing in vivo. *npj Flex. Electron* **4**, 5 (2020).
24. Marion, J. S. et al. Thermally drawn highly conductive fibers with controlled elasticity. *Adv. Mater.* **34**, 2201081 (2022).
25. Qu, Y. et al. Superelastic multimaterial electronic and photonic fibers and devices via thermal drawing. *Adv. Mater.* **30**, 1707251 (2018).
26. Dong, C. et al. High-efficiency super-elastic liquid metal based triboelectric fibers and textiles. *Nat. Commun.* **11**, 3537 (2020).
27. Jin, H. et al. Highly durable nanofiber-reinforced elastic conductors for skin-tight electronic textiles. *ACS Nano* **13**, 7905–7912 (2019).
28. Yan, W. et al. Single fibre enables acoustic fabrics via nanometre-scale vibrations. *Nature* **603**, 616–623 (2022).
29. Li, B. M. et al. Influence of armband form factors on wearable ECG monitoring performance. *IEEE Sens J.* **21**, 11046–11060 (2021).
30. Wang, L. et al. Weaving sensing fibers into electrochemical fabric for real-time health monitoring. *Adv. Funct. Mater.* **28**, 1804456 (2018).
31. Jin, H. et al. Enhancing the performance of stretchable conductors for E-textiles by controlled ink permeation. *Adv. Mater.* **29**, 1605848 (2017).
32. Yapici, M. K., Alkhidir, T., Samad, Y. A. & Liao, K. Graphene-clad textile electrodes for electrocardiogram monitoring. *Sens Actuators B Chem.* **221**, 1469–1474 (2015).
33. Wang, C. et al. Advanced carbon for flexible and wearable electronics. *Adv. Mater.* **31**, 1801072 (2019).
34. Trovato, V. et al. Sol-gel approach to incorporate millimeter-long carbon nanotubes into fabrics for the development of electrical-conductive textiles. *Mater. Chem. Phys.* **240**, 122218 (2020).
35. Yang, J. C. et al. Electronic skin: recent progress and future prospects for skin-attachable devices for health monitoring, robotics, and prosthetics. *Adv. Mater.* **31**, 1904765 (2019).
36. Lee, S. M. et al. Self-adhesive epidermal carbon nanotube electronics for tether-free long-term continuous recording of biosignals. *Sci. Rep.* **4**, 6074 (2014).
37. Liu, B. et al. Wearable carbon nanotubes-based polymer electrodes for ambulatory electrocardiographic measurements. *Sens Actuators A Phys.* **265**, 79–85 (2017).
38. Liu, B., Luo, Z., Zhang, W., Tu, Q. & Jin, X. Silver nanowire-composite electrodes for long-term electrocardiogram measurements. *Sens Actuators A Phys.* **247**, 459–464 (2016).
39. Koo, J. H. et al. Wearable electrocardiogram monitor using carbon nanotube electronics and color-tunable organic light-emitting diodes. *ACS Nano* **11**, 10032–10041 (2017).
40. Li, B. M. et al. Iron-on carbon nanotube (CNT) thin films for biosensing E-textile applications. *Carbon N. Y* **168**, 673–683 (2020).
41. Taylor, L. W. et al. Washable, sewable, all-carbon electrodes and signal wires for electronic clothing. *Nano Lett.* **21**, 7093–7099 (2021).
42. Tang, Y. et al. Cotton-based naturally wearable power source for self-powered personal electronics. *J. Mater. Sci.* **55**, 2462–2470 (2020).
43. Anike, J. C., Belay, K. & Abot, J. L. Effect of twist on the electromechanical properties of carbon nanotube yarns. *Carbon N. Y* **142**, 491–503 (2019).
44. Cherenack, K., Zysset, C., Kinkeldei, T., Münzenrieder, N. & Tröster, G. Woven electronic fibers with sensing and display functions for smart textiles. *Adv. Mater.* **22**, 5178–5182 (2010).
45. Zhao, J. et al. Double-peak mechanical properties of carbon-nanotube fibers. *Small* **6**, 2612–2617 (2010).
46. Hill, F. A., Havel, T. F., Hart, A. J. & Livermore, C. Enhancing the tensile properties of continuous millimeter-scale carbon nanotube fibers by densification. *ACS Appl Mater. Interfaces* **5**, 7198–7207 (2013).
47. Bai, Y. et al. Carbon nanotube bundles with tensile strength over 80 GPa. *Nat. Nanotechnol.* **13**, 589–595 (2018).
48. Uzun, S. et al. Knittable and washable multifunctional MXene-coated cellulose yarns. *Adv. Funct. Mater.* **29**, 1905015 (2019).
49. Maziz, A. et al. Knitting and weaving artificial muscles. *Sci. Adv.* **3**, e1600327 (2017).

50. Ji, F., Li, R. & Qiu, Y. Simulate the dynamic draping behavior of woven and knitted fabrics. *J. Ind. Text.* **35**, 201–215 (2006).
51. Au, K. in *Advances in Knitting Technology* (ed. Au, K. F.) 213–232 (Woodhead, 2011).
52. Xu, W., Chen, Y., Zhan, H. & Wang, J. N. High-strength carbon nanotube film from improving alignment and densification. *Nano Lett.* **16**, 946–952 (2016).
53. Luo, X. et al. Multifunctional fabrics of carbon nanotube fibers. *J. Mater. Chem. A* **7**, 8790–8797 (2019).
54. Pani, D., Achilli, A. & Bonfiglio, A. Survey on textile electrode technologies for electrocardiographic (ECG) monitoring, from metal wires to polymers. *Adv. Mater. Technol.* **3**, 1800008 (2018).
55. Ankhili, A. et al. Comparative study on conductive knitted fabric electrodes for long-term electrocardiography monitoring: Silver-plated and PEDOT:PSS coated fabrics. *Sens. (Switz.)* **18**, 3890 (2018).
56. O'Mahony, C. et al. Design, fabrication and skin-electrode contact analysis of polymer microneedle-based ECG electrodes. *J. Micromech. Microeng.* **26**, 084005 (2016).
57. Alizadeh-Meghrazi, M. et al. Evaluation of dry textile electrodes for long-term electrocardiographic monitoring. *Biomed. Eng. Online* **20**, 68 (2021).
58. Takeshita, T. et al. Relationship between contact pressure and motion artifacts in ECG measurement with electrostatic flocked electrodes fabricated on textile. *Sci. Rep.* **9**, 5897 (2019).
59. Yokus, M. A. & Jur, J. S. Fabric-based wearable dry electrodes for body surface biopotential recording. *IEEE Trans. Biomed. Eng.* **63**, 423–430 (2016).
60. Xu, X., Luo, M., He, P. & Yang, J. Washable and flexible screen printed graphene electrode on textiles for wearable healthcare monitoring. *J. Phys. D. Appl Phys.* **53**, 125402 (2020).
61. Zhou, W. et al. Fabrication and impedance measurement of novel metal dry bioelectrode. *Sens Actuators A Phys.* **201**, 127–133 (2013).
62. Yu, Q. et al. ECG R-wave peaks marking with simultaneously recorded continuous blood pressure. *PLoS One* **14**, e0214443 (2019).
63. Li, B. M. et al. Textile-integrated liquid metal electrodes for electrophysiological monitoring. *Adv. Healthc. Mater.* **11**, 2200745 (2022).
64. Afroj, S., Tan, S., Abdelkader, A. M., Novoselov, K. S. & Karim, N. Highly conductive, scalable, and machine washable graphene-based E-textiles for multifunctional wearable electronic applications. *Adv. Funct. Mater.* **30**, 2000293 (2020).
65. Aly, K., Li, A. & Bradford, P. D. Strain sensing in composites using aligned carbon nanotube sheets embedded in the interlaminar region. *Compos Part A Appl Sci. Manuf.* **90**, 536–548 (2016).
66. He, N. et al. Pyrolytic-carbon coating in carbon nanotube foams for better performance in supercapacitors. *J. Power Sources* **343**, 492–501 (2017).
67. Aly, K. & Bradford, P. D. Real-time impact damage sensing and localization in composites through embedded aligned carbon nanotube sheets. *Compos B Eng.* **162**, 522–531 (2019).
68. The American Association of Textile Chemists and Colorists. AATCC Technical Manual. Research Triangle Park, NC, USA. Test Method 61–2013: Colorfastness to laundering: Accelerated; 86–90 (2011).

ACKNOWLEDGEMENTS

This work was supported by the Analytical Instrumentation Facility (AIF) at North Carolina State University, which is supported by the State of North Carolina and the National Science Foundation (award number ECCS-1542015). The authors acknowledge the US Department of Defense (DoD) and the Air Force Life Cycle Management Center (AFLCMC) for provision of the Science Mathematics and Research for Transformation (SMART) scholarship to B.M.L. We would like to thank Patrapee Kungsadalpipob for helping with the electromechanical testing of the electrodes.

AUTHOR CONTRIBUTIONS

All authors contributed to the writing and editing of this manuscript. M.M.H. and P.B. conceived the original ideas presented in this work and P.B. supervised the overall project. M.M.H. synthesized CNTs and fabricated the freestanding ECG sensor. M.M.H., B.M.L., and B.S. performed material characterization, ECG and impedance data acquisition, analysis and visualization. J.J. provided technical guidance on ECG measurements and supported supervision of this project. All authors discussed the results and commented on the manuscript.

COMPETING INTERESTS

The authors declare no competing interests.

ADDITIONAL INFORMATION

Supplementary information The online version contains supplementary material available at https://doi.org/10.1038/s41528-022-00230-3.

Correspondence and requests for materials should be addressed to Philip D. Bradford.

Reprints and permission information is available at http://www.nature.com/reprints

Publisher's note Springer Nature remains neutral with regard to jurisdictional claims in published maps and institutional affiliations.